

Formation of petroleum organic deposits on steel surfaces

A. Cosultchi,^{1,2*} A. García-Bórquez,³ J. Aguilar-Hernandez,³ H. Yee-Madeira,^{3†} E. Reguera,⁴ V. H. Lara⁵ and P. Bosch⁵

¹ Dept. of Metallurgical Engineering, ESQIE-IPN, 07738 Mexico City, Mexico

² Instituto Mexicano del Petroleo, 07730 Mexico City, Mexico

³ ESFM-IPN, 07738, Mexico City, Mexico

⁴ Universidad de La Habana, Cuba

⁵ UAM-Iztapalapa, 09340, Mexico City, Mexico

Received 16 July 2001; Revised 30 November 2001; Accepted 24 December 2001

An adhered organic deposit, formed within the petroleum well on the steel surface of the tubing walls, was systematically characterized following a sequence of bulk and surface techniques. The results allowed the identification of the tubing wall and its internal surface structures. As a consequence of the contact with sulphur-bearing compounds such as H₂S and brine from petroleum, the pre-oxidized steel surface was modified by non-stoichiometric iron compound formation. These new iron phases favour adsorption and chemisorption of the petroleum polar compounds on the steel surface. Copyright © 2002 John Wiley & Sons, Ltd.

KEYWORDS: petroleum well; carbon steel surface; adherence; SEM-EDS; AES; XRD; Mössbauer; FTIR; Raman; spectroscopy

INTRODUCTION

When materials such as steel are exposed to multicomponent environments, as in the petroleum well, several processes such as oxidation, sulphidation or carburization may occur not only at the gas/metal interface but also within the scale that preserves the reaction products.¹ In addition to the new iron phases formed in such an environment, organic material was found adhered on the internal surface of some petroleum wells.² The study of this material is difficult, because the adhered layer is irregular and consequently the compositional information obtained only by means of surface-specific techniques could be incomplete. For instance, the type of carbon steel used for the tubing and its manufacturing process could affect the tubing wall composition and structure. In addition, the hydrocarbon ambient modifies the steel surface³ and, furthermore, its complexity increases when the internal surface of the tubing is petroleum- or brine-wetted. Moreover, extraction of the tubing piece from the well implicated the formation of other iron compounds as a consequence of its exposure to the atmosphere.⁴

In this work, the identification of elements, their chemical bonding and concentrations as well as the particular morphologies observed in the bulk structure and on the tubing border was carried out by means of several bulk and

surface-specific techniques. Additionally, a discussion concerning the interpretation of results as well as mechanisms of formation of the identified compounds is presented.

EXPERIMENTAL

Metallic coupons with an adhered layer of black material were cut from a piece of tubing removed from a Mexican well. A cross-section of a metallic coupon was polished and prepared for microscopic observations by gold coating. Energy-dispersive spectroscopy (EDS; Jeol JSM 6300 with Noran Microanalyst spectrometer at 15 kV and a working distance of 39 mm) and Auger electron spectroscopy (AES; Jeol JAMP 30 at 10 kV) registered the chemical compositions across the wall section of the tubing.⁵ These techniques also provide elemental compositions at different depths. Auger spectra of the sample were registered after sputtering with argon. Element quantification was accomplished using sensitivity factors from the literature.⁶ Fourier transform infrared (FTIR; Perkin-Elmer 2000 FT-IR) and Raman spectroscopies in reflection mode, as well as x-ray diffraction (D500 Siemens diffractometer with Cu K_α source) results were acquired from the surface with the adhered layer. The Raman spectrum was obtained with the 514.5 nm line of an Ar⁺ laser (40 mW) focused to an area of ~0.5 mm². The outcoming radiation was analysed by a double monochromator (1403-SPEX) and detected by a thermoelectrically cooled photomultiplier tube (RCA-C3104) connected to a photon counting system.

Additionally, Mössbauer spectroscopy was applied to the scraped powder of the steel surface in order to

*Correspondence to: A. Cosultchi, Instituto Mexicano del Petroleo, 152 Eje Central "L. Cardenas," Mexico City 07730, Mexico.

E-mail: acosul@imp

Contract/grant sponsor: Instituto Mexicano del Petroleo;

Contract/grant number: FIES 97-06-I.

†CO FAA Fellow

identify the iron phases and their oxidation state. Elemental composition by combustion (Elemental Vario EL and Leco SC-44) was applied to the scraped material, whereas the bulk steel composition was obtained by atomic absorption spectroscopy (AAS; Perkin-Elmer 5000).

RESULTS

Figure 1 shows part of the coupon wall and the coupon border of the steel tubing. The coupon border displays a very irregular morphology with 'valley' and 'chain-like' structures, B1 and B2, respectively. The bulk metal composition obtained by AAS is presented in Table 1 and compared with the API standard composition.⁷ Table 2 presents the bulk and surface compositions registered by EDS and AES across the tubing wall section from the zones indicated in Fig. 1.

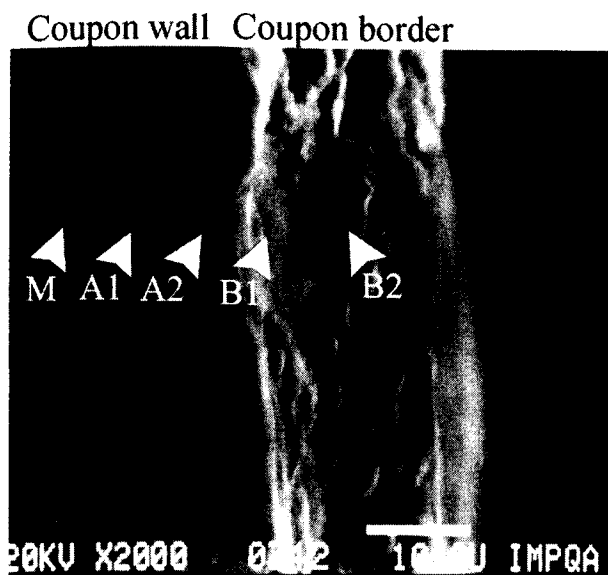


Figure 1. Cross-section micrograph of a steel coupon sectioned from a petroleum-tubing piece with an irregular border, showing the EDS and AES spectra registration zones.

Table 1. Elemental composition of a tubing steel coupon obtained by atomic absorption spectroscopy (AAS) and the API compositions

Element	AAS results (wt.%)	API specification for L-80 type Tubing	
		L-80/1(wt.%)	L-80/2(wt.%)
Fe	97.39	95.56	87.47
Mn	0.80	1.9	0.60
Cr	0.20	—	10.00
Ni	0.07	0.25	0.50
Cu	0.22	0.35	0.25
Mo	0.05	—	—
Si	0.37	0.45	1.00
C	0.90	0.49	0.18
P	0.90	0.49	0.18
S	0.90	0.49	0.18

Chromium and molybdenum were identified by AES in the metal composition (zone M), whereas the EDS results indicate only a very small amount of chromium on the coupon border (zone A2). Auger electron spectroscopy registered the highest amount of silicon in zone A1, whereas by EDS the highest silicon amount was detected in zone B1. The highest amounts of sulphur and carbon were detected by AES at zone B1. Additionally, other elements registered on the coupon border by EDS and AES (Table 1) are particularly associated to the valley-like morphology.

On the other hand, the adhered material scraped from the steel surface contained C, H, O, N, S and metals, with 85.62, 7.14, 0.71, 0.51, 6.19 and 2.84 wt.%, respectively, as the combustion and AAS results show. The AAS-identified metals were Fe, Ca, Ba, Na, V, Si, Mg and Ni, with 2.29, 0.14, 0.10, 0.09, 0.07, 0.07, 0.02 and 0.01 wt.%, respectively. Most of these metals were petroleum reservoir endogenous minerals such as NaCl, silicates and CaCO₃ and exogenous minerals such as BaSO₄.⁸

The crystallographic information on the surface adhered layer was resolved by x-ray diffraction and presented

Table 2. Bulk (EDS) and surface (AES) elemental compositions of the steel cross-section (at.%)

Element	EDS					Element	AES				
	M	A1	A2	B1	B2		M	A1	A2	B1	B2
Fe	95.8	55.4	57.3	45.1	59.1	Fe	30.3	6.2	4.1	2.3	7.5
O	1.9	43.2	40.9	34.7	27.7	O	58.9	66.6	82.4	27.5	52.7
Mn	1.5	1.0	0.8	0.8	1.0	Mn	3.9	1.8	1.0	0	0
Si	0.7	0.4	0.7	2.8	0.4	Si	0	1.7	1.0	0	0
S	—	—	—	—	6.9	S	0	0	5.4	23.5	15.0
C	—	—	—	7.9	3.7	C	0	23.7	6.1	44.3	24.8
Cr	—	—	0.2	0.1	0.1	Cr	5.2	—	—	—	—
Al	—	—	0.2	7.0	0.3	Mo	1.7	—	—	—	—
Ca	—	—	—	0.6	0.2	Al	—	—	—	—	—
Cl	—	—	—	0.2	0.3	Ca	—	—	—	2.4	—
Na	—	—	—	—	0.3						
K	—	—	—	0.9	—						

in Fig. 2. Magnetite crystals (JCPDS 11-0614) identified on the coupon surface exhibited preferential orientation towards the direction of the most intense peak (311), whereas pyrrhotite crystals (JCPDS 22-0358) did not exhibit any preferential orientation.³ Small peaks of iron oxide hydroxide (lepidocrocite, JCPDS 44-1415), which did not maintain the intensities of the JCPDS pattern, were also identified. In addition, Mössbauer spectroscopy of the adhered material scraped from the steel surface (Table 3) revealed that magnetite has an electronic structure similar to a disordered maghemite with the following stoichiometry: $(\text{Fe}^{3+})(\text{Fe}_{1+2x}^{3+}\text{Fe}_{1-3x}^{2+}\text{O}_4)$ (where $x \sim 0.03$). Pyrrhotite with a low stoichiometry, Fe_{1-x}S (where $x \sim 0.125$), as well as goethite ($\alpha\text{-FeOOH}$) and lepidocrocite ($\gamma\text{-FeOOH}$) were also identified.

Figure 3 shows that the FTIR spectrum is dominated by aliphatic chain vibration bands. The $\nu\text{-CH}_3$ asymmetric vibration band at 2960 cm^{-1} has a high intensity and the $\delta\text{-CH}_3$ symmetric vibration band is raised to 1464 cm^{-1} , the upper limit, which indicates electronegative substituents.⁹ The small band at 2733 cm^{-1} corresponds to the stretching vibration of the N-CH_3 group.⁹ The Raman spectrum shown in Fig. 2(b) establishes seven peaks at $3058, 2985, 2955, 2836, 2760, 2725$ and 2651 cm^{-1} after the signal was deconvoluted by mean of the Microcal Origin Peak Fitting Module. These peaks corresponds to the following functional groups: cyclic alkenes, O-CH_3 (asym.), O-CH_2 (sym.), O-CH_3 (sym.), $-\text{COH}$, $\text{O-CH}_2\text{-O}$ and $-\text{NH}_x^+$ cations,⁹ respectively.

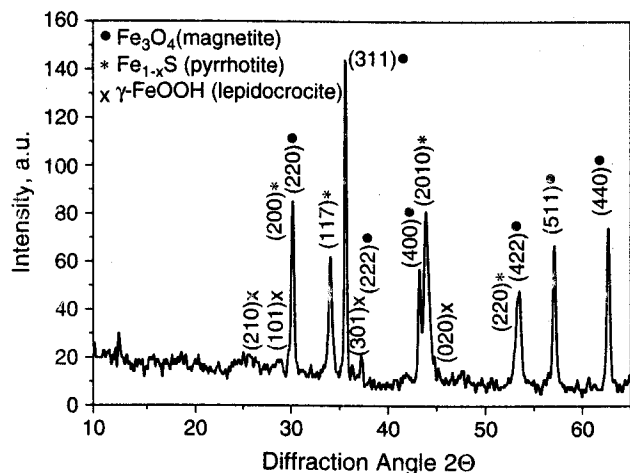


Figure 2. X-ray diffractogram of the tubing surface.

In addition, the 1690 cm^{-1} vibration band in the FTIR spectrum indicates the occurrence of carbonyl groups. On the other hand, bands within the range $3440\text{--}3208\text{ cm}^{-1}$ are related to amine, free OH and hydroxyl groups bonded to the surface, whereas the vibration bands at 1320 and 1033 cm^{-1} might correspond to $\delta_{\text{O-H}}$ and $\nu_{\text{C-O}}$ in hydroxyl groups.⁹

DISCUSSION

The mean elemental composition of a tubing piece obtained by AAS spectroscopy indicates that, according to the API standard,⁷ the material type is L-80/I, although additionally it contains small amounts of Cr, Ni and Mo.

Apparently, processes such as oxidation and sulphidation were promoted mainly on the internal tubing surface by steps. Magnetite has to be considered as part of the previous protective layer developed during the manufacturing thermal process. Non-stoichiometric iron compounds such as pyrrhotite and maghemite were materialized on the pre-oxidized steel surface after its exposure to the sulphur-hydrocarbon-brine ambient. The immediate precursors of these compounds are assumed to be lepidocrocite, amorphous ferrihydrite and elemental iron,¹⁰ although chemisorption of H_2S molecules on Fe^{2+} sites is not excluded.¹¹

Although petroleum contains small amounts of brine in addition to the corrosive gases CO_2 and H_2S , water molecules are chemisorbed and dissociated on the iron oxide surface, promoting Brønsted acidic and basic sites but not the formation of new iron phases.¹² Moreover, the oxidized magnetite conserves the cubic structure, which also indicates lepidocrocite as an intermediary phase.¹³ However, lepidocrocite ($\gamma\text{-FeOOH}$) and goethite ($\alpha\text{-FeOOH}$), identified by Mössbauer spectroscopy, were eventually formed only after the tubing was exposed to atmosphere moisture.^{3,14,15}

The locally high amount of silicon registered by AES and EDS indicates the formation of irregular sections of occluded silicon oxide (SiO_2). This compound only should be the result of the manufacturing process, because the petroleum well temperature is minor compared to 850°C , which is the temperature of the silica layer formation.¹⁶ Additionally, the high amount of carbon registered by AES in zone A1 also suggests the segregation of this element from bulk steel.¹

The tubing internal surface is highly irregular, with valley and chain-like structures indicated in Fig. 1 as zones B1 and B2. The AES results indicate that zone B1 contains less Fe and more S, C and Ca than zone B2. Additionally, in zone B1 the O/Fe atomic ratio is higher than in zone B2. The AES

Table 3. Mössbauer parameters of the surface scraped layer recorded at room temperature

Assignment	δ (mm s^{-1})	Δ (mm/s^{-1})	H_f (T)	Relative area (%)	Normalized area (%)
Magnetite (Fe_3O_4)(A)	0.29	0	490	25	1.50
Magnetite (Fe_3O_4)(B)	0.63	0	453	11	0.66
Goethite ($\alpha\text{-FeOOH}$)	0.33	-0.19	260	24	1.44
Lepidocrocite ($\gamma\text{-FeOOH}$)	0.30	0.59	0	22	1.32
Pyrrhotite (Fe_{1-x}S)	0.80	0.06	310	18	1.08

Symbols: δ is the isomer shift value relative to $\alpha\text{-Fe}$; Δ is the quadrupolar splitting; H_f is the magnetic field intensity; (A) indicates the tetrahedral sites of Fe(III) and (B) the octahedral sites of Fe(II/III).

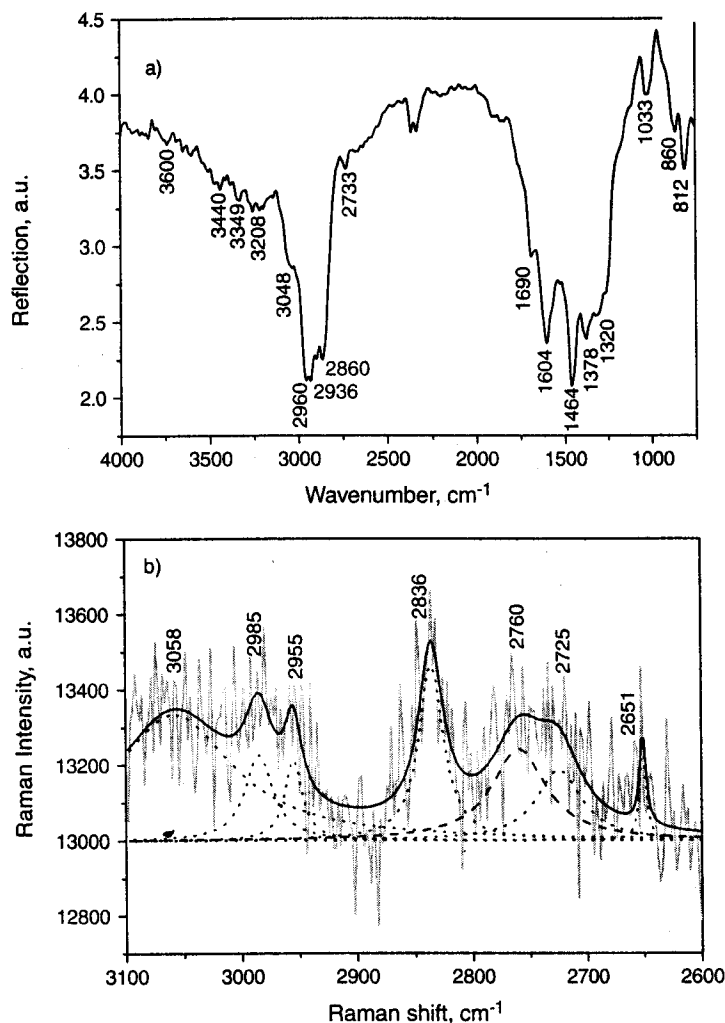


Figure 3. (a) Infrared spectrum of the steel surface recorded in reflection mode (4000–700 cm^{-1}). (b) Raman spectrum of the steel surface recorded in reflection mode (3100–2600 cm^{-1}), showing the fitted peaks.

spectrum of zone B1 reveals the presence of other types of sulphur compounds than iron sulphide. The position of the Fe KLL signals in this AES spectrum indeed suggests only the presence of iron oxides. Therefore, the most probable sulphur compound is barite (BaSO_4), which is a drilling well ingredient, although barium was not detected. The high amount of carbon registered by EDS and AES in zone B2 could be associated with organic or carbonate compounds such as calcite or aragonite (CaCO_3). Moreover, the AES spectrum indicates other iron compounds and a low iron oxidation degree. Therefore, pyrrhotite (Fe_{1-x}S) is the most probable iron compound.

Specific chemisorption of the organic compounds on the steel surface is very complex, although the *in situ* transformation of the steel surface and non-stoichiometric iron compound formation favour this process. Molecules with high donor orbital energy are strongly bonded to a surface with low acceptor orbital energy.¹⁷ Consequently, the strength of the surface bond is directly correlated to the electronegativity of the functional group of the organic molecules. Thus, molecules with localized lone-pair electrons chemisorb strongly on the oxidized iron surface, whereas molecules with delocalized electrons (such as π -electrons)

adsorb molecularly without dissociation.¹⁸ In this work, the presence of cyclic alkene, functional groups (carbonyl, ether, hydroxyl and ammonium salt) and organometallic compounds of Ni and V could be explained via this mechanism.

Additionally, the reported intensity of the methyl symmetric stretching vibration at 2860 cm^{-1} indicates that aliphatic chains are oriented towards the tubing surface, either parallel or perpendicular to it. For example, an aromatic ring such as ethylbenzene, which is a soft basic aromatic petroleum compound, is chemisorbed on the acidic iron sites of Fe_3O_4 or Fe_2O_3 surfaces. The side-chain is bent out of the plane and hydrogen atoms interact with surface oxygen sites.¹⁷ However, although there is high coverage of the iron oxide surfaces by such compound types, it is difficult to explain the thickness of a real adhered layer. In that case, other aspects such as surface roughness and mineral particles should be evaluated.

CONCLUSIONS

The results allowed the differentiation between compounds produced during the tubing steel manufacturing, those formed on the tubing surface as a consequence of petroleum

contact and those compounds formed after the steel was extracted from the petroleum well and exposed to the atmosphere. Consequently, the systematic characterization of a tubing steel coupon indicates that the original oxide layer experienced *in situ* phase transformation and the formation of non-stoichiometric compounds when it is wetted by petroleum under the well's operating conditions. This step is considered as the foregoing condition to the chemisorption of both polar molecules and mineral compounds from petroleum flow on the tubing steel surface. On the contrary, iron oxide hydroxide is formed when the tubing surface is wetted by water.

Acknowledgement

This research was supported by Instituto Mexicano del Petroleo (Grant no. FIES 97-06-I).

REFERENCES

1. Natesan K. In *Oxidation of Metals and Associated Mass Transport*, Norman L. Peterson Memorial Symposium. Metallurgic Society: 1986.
2. Cosultchi A, Garciafigueroa E, Muñoz A, Zeifert B, Garcia-Borquez A, Lara VH, Bosch P. *Surf. Rev. Lett.* 1999; **6**: 1299.
3. Ramanarayanan TA, Smith SN. *Corrosion* 1998; **46**: 66.
4. Evans UR. *The Corrosion and Oxidation of Metals*. Edward Arnold: London, 1976.
5. Brandon D, Kaplan WD. *Microstructural Characterization of Materials*. John Wiley: Chichester, 1999.
6. Davis EL, MacDonald NC, Palmberg PW, Riach GE, Weber RE. *Handbook of Auger Electron Spectroscopy*. Physical Electronic Industries: Eden Prairie, MN, 1976.
7. *API Specification 5CT: Specification for Casing and Tubing*. American Petroleum Institute: Washington, 1995.
8. Cosultchi A, Garciafigueroa E, Mar B, García-Bórquez A, Lara VH, Bosch P. *Fuel* 2002; **81**(4): 413–421.
9. Socrates G. *Infrared Characteristic Group Frequencies* (2nd edn). John Wiley: Chichester, 1997.
10. Kaneko T, Tazawa K, Koyama T, Satou K, Shimazaki K, Kageyama Y. *Energy Fuels* 1998; **12**: 897.
11. Rodriguez JA, Hrbek J. *Acc. Chem. Res.* 1999; **32**: 719.
12. Kung HH. *Transition Oxide Metal: Surface Chemistry and Catalysis. Studies in Surface Science and Catalysis*, vol. 45. Elsevier: Amsterdam, 1989.
13. Diakonov II. *Eur. J. Miner.* 1998; **10**: 17.
14. Laberty C, Navrotsky A. *Geochim. Cosmochim. Acta* 1998; **62**: 2905.
15. Cosultchi A, Garciafigueroa E, Reguera E, Yee-Madeira H, García-Bórquez A, Zeifert B, Lara VH, Bosch P. *Fuel* 2001; **80**: 1963.
16. Robertson J, Manning MI. *Mater. Sci. Technol.* 1989; **5**: 741.
17. Joseph Y, Wühn M, Niklewski A, Ranke W, Weiss W, Wöll C, Schlögl R. *Phys. Chem. Chem. Phys.* 2000; **2**: 5314.
18. Pan FM, Stair PC, Fleisch TH. *Surf. Sci.* 1986; **177**: 1.